



OPEN

# High performance catalytic distillation using CNTs-based holistic catalyst for production of high quality biodiesel

SUBJECT AREAS:

HETEROGENEOUS  
CATALYSISMATERIALS FOR ENERGY AND  
CATALYSIS

RENEWABLE ENERGY

Dongdong Zhang<sup>1\*</sup>, Dali Wei<sup>1\*</sup>, Qi Li<sup>1</sup>, Xin Ge<sup>1</sup>, Xuefeng Guo<sup>1</sup>, Zaiku Xie<sup>2</sup> & Weiping Ding<sup>1</sup><sup>1</sup>Key Lab of Mesoscopic Chemistry, the School of Chemistry and Chemical Engineering, Nanjing University, Nanjing 210093, China, <sup>2</sup>Shanghai Research Institute of Petrochemical Technology, Shanghai 201208, China.Received  
29 November 2013Accepted  
14 January 2014Published  
7 February 2014Correspondence and  
requests for materials  
should be addressed to  
W.P.D. (Dingwp@nju.  
edu.cn)\* These authors  
contributed equally to  
this work.

For production of biodiesel from bio oils by heterogeneous catalysis, high performance catalysts of transesterification and the further utilization of glycerol have been the two points of research. The process seemed easy, however, has never been well established. Here we report a novel design of catalytic distillation using hierarchically integrated CNTs-based holistic catalyst to figure out the two points in one process, which shows high performance both for the conversion of bio oils to biodiesel and, unexpectedly, for the conversion of glycerol to more valuable chemicals at the same time. The method, with integration of nano, meso to macro reactor, has overwhelming advantages over common technologies using liquid acids or bases to catalyze the reactions, which suffer from the high cost of separation and unsolved utilization of glycerol.

Biodiesel made from bio oils, as a kind of high quality fuel, has drawn much more research attentions in recent years<sup>1-3</sup>. High performance transesterification process and the treatment of main by-product glycerol have been the two points of research. Commonly, liquid acids or bases are used to catalyze transesterification and esterification reactions<sup>4-6</sup>, which suffer from the largely excess quantity of methanol needed to remove equilibration limit on conversion and the high cost of separation<sup>7-9</sup>. And the utilization of glycerol, as main by-product, is still a question. Some heterogeneous catalysts used for the reaction have been developed, including KOH/Al<sub>2</sub>O<sub>3</sub><sup>10</sup>, Al<sub>2</sub>O<sub>3</sub>/SnO<sub>2</sub><sup>11</sup>, Li/MgO<sup>12</sup>, Amberlyst-15<sup>13</sup>, Nafion<sup>14</sup>, and zeolites<sup>15</sup>. These processes using solid catalysts, however, demand rigorous conditions, such as free of dissociative fatty acids<sup>16-18</sup>. And recently, carbon-based solid acids have been reported promising to catalyze reactions of esterification or transesterification to produce biodiesel<sup>19-25</sup>. Considering the big advantages of catalytic distillation as intensified processes for the highly efficient couple of reactions and separation, some investigators have reported on the implementation of a reactive distillation to biodiesel production with acidic resin Amberlyst-15 or sodium hydroxide as catalysts<sup>26,27</sup>. The general performances of these catalysts, however, are still much inferior to the demand.

In this report, a continuous catalytic distillation process using shaped holistic catalysts with CNTs grown on stainless steel wire mesh has been developed and shown high performance for transesterification of bio oils with methanol and surprisingly also for the synchronous conversion of glycerol to high valued products. The catalytic distillation apparatus for the research purpose is schematically shown as Fig. 1. Firstly, the carbon nanotubes were tightly grown on the steel wires of the mesh and then the mesh was shaped as Raschig rings (diameter: 2 mm, length 2 mm). After sulfonation, the Raschig rings were loaded in a catalytic distillation column (height: 200 mm, diameter: 20 mm). The transesterification of bio oils with methanol was carried out using the distillation column at 493 K in high efficiency, due to the simultaneous separation removing the limitation of chemical equilibrium. Unexpectedly, the glycerol, as the by product of the reaction in common processes, was found simultaneously to convert to a series of higher valuable compounds over the catalytic column, which would extremely promoted the performance of the process scientifically and economically.

## Results

**Preparation of the holistic catalyst.** Fig. 2a shows the photograph of the fresh stainless steel mesh with the wires in diameter of 200  $\mu\text{m}$ . Before the CNTs' growth, the metallic cobalt nanoparticles, synthesized according to ref. 28, have been coated to the wires as catalysts for CNTs rooted on the wires (inset). Fig. 2b depicts the stainless steel mesh with thickly grown CNTs and the Raschig rings made from the stainless steel mesh (inset). Fig. 2c shows the compact and orderly CNTs' array on the wires with the length of CNTs about  $\sim 30 \mu\text{m}$ . The carbon nanotubes are in good shape of one dimensional morphology and the metallic particles of catalyst, cobalt and iron, are evidently

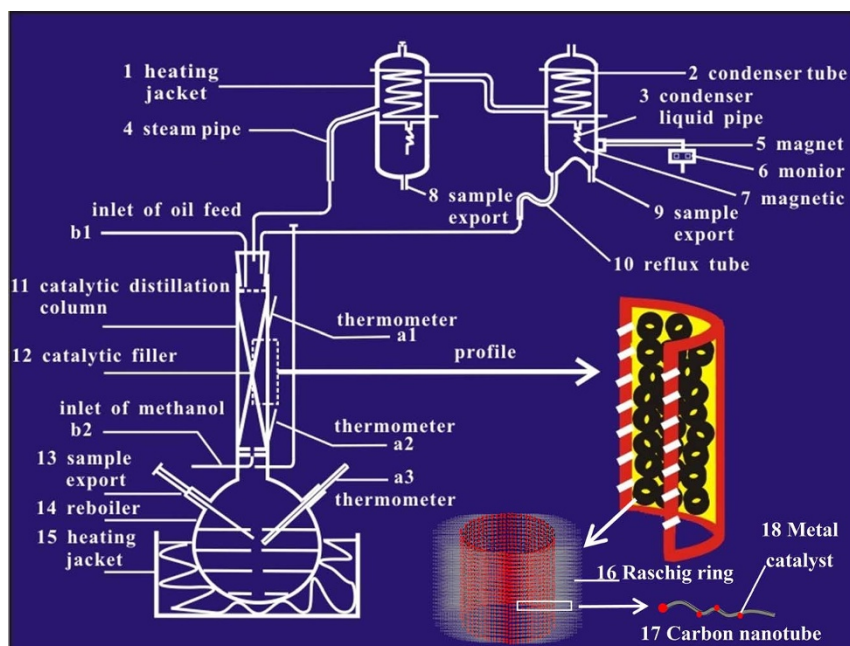


**Figure 1** | The schematic show of the catalytic distillation apparatus for the transesterification of bio oils and the synchronous conversion of glycerol to high valuable products.

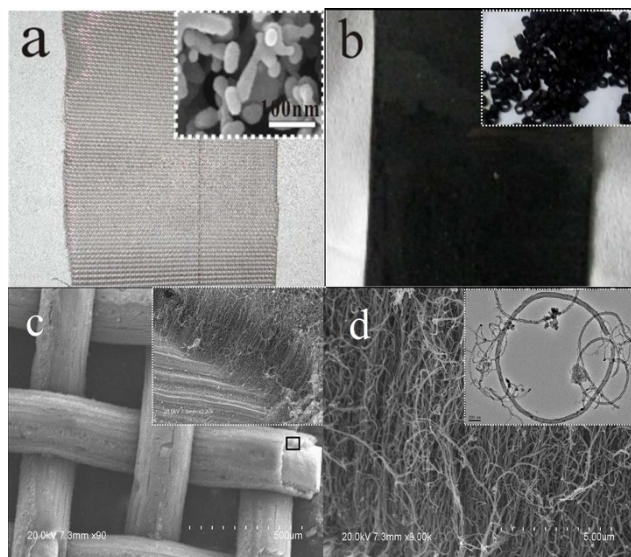
clued or embedded in the carbon nanotube along its length (Fig. 2d)<sup>29</sup>. The metal nanoparticles would be also included in catalytic reactions.

The CNTs on the Rashig rings are sulfurated with  $\text{Na}_2\text{S}_x$  and oxidized by hydrogen peroxide to sulfonic acid. After the chemical treatment, the carbon nanotubes arrays on the wires are still in similar to the original steel mesh (Figs. 3a and 3b). The Raman spectra of

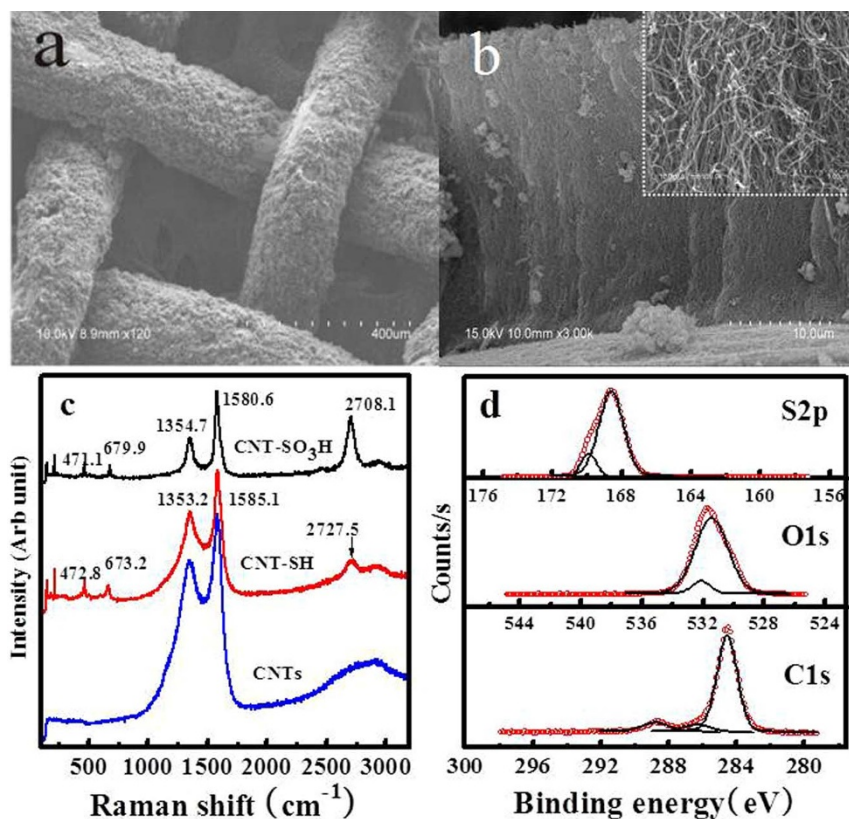
original and chemically treated CNTs are shown in Fig. 3c. The bands at  $\sim 1356$  and  $\sim 1585$   $\text{cm}^{-1}$  are the characteristic D-band and G-band of graphite carbon, respectively. The G-band is attributed to the tangential mode of the graphitic structure, while D-band corresponds to the defects or limited dimensions of CNT crystal structure<sup>30</sup>. The intensity of the G-band is stronger than the D-band, indicating the high degree of graphitization. For the sample of CNT-SH, new peaks at 472, 673 and 2727  $\text{cm}^{-1}$  are observed. The peak at 472  $\text{cm}^{-1}$  is associated with bend vibrations of S=C-S bonds<sup>31</sup>, the 673  $\text{cm}^{-1}$  peak is related to stretch vibrations of C-S bonds<sup>9,31,32</sup>, while the 2727  $\text{cm}^{-1}$  band is stretch vibrations of S-H bonds<sup>33</sup>. For the sample after oxidation with CNT-SO<sub>3</sub>H groups, the peak at 2708  $\text{cm}^{-1}$  from stretching vibrations of O-H bonds in sulfonic group arises<sup>34</sup>.

Figure 3d showed XPS spectra of the sulfonated CNTs-based structured catalyst. Three peaks, respectively positioned at 284.5, 286.3, and 288.7 eV, are observed in the C1s region. The peak centered at 284.5 eV can be attributed to the  $\text{sp}^2$ - hybridized graphite carbon. The peak at 286.3 eV is contributed from carbon atoms in the C-O- species<sup>35</sup>. The peak at 288.7 eV is associated with the carbon atoms in C-S species<sup>36</sup>. The O1s binding energy can be deconvoluted into two peaks at 531.5 and 532.1 eV, which are assigned as oxygen atoms in S-OH and C-OH, respectively. In the region of S2p, two peaks appeared at 168.5 and 169.7 eV are detected, which are assigned to the -SO<sub>3</sub>H groups in the sample<sup>37</sup>. The chemical composition of the holistic catalyst analyzed by EDX equipped to the scanned electron microscopy is listed in Table 1 and the effective protonic acid density attached to the CNTs measured by titration is also listed in table 1. The results confirm the high content of sulfur in the catalyst. After oxidation treatment, the oxygen content increases remarkably and implies the existence of groups of -COOH and -OH, besides the groups of -SO<sub>3</sub>H. The acid density of 2.54  $\text{mmol}\cdot\text{g}^{-1}$  is a medium-high value among the carbon-based solid acids documented.

**Catalytic distillation process for bio oil conversion.** The Rashig rings are loaded as fillers into a catalytic distillation column, 20 mm in diameter and 200 mm in height. The total amount of CNTs grown on the Rashig rings is  $\sim 2.1$  g with total surface area about 450  $\text{m}^2$ . During catalytic operation, the reactive mixtures of



**Figure 2** | The stainless steel meshes and the cobalt nanoparticles coated onto the meshes (SEM, inset); (b) The stainless steel meshes after CNTs growth and the Raschig rings (inset); (c) SEM image of stainless steel mesh coated with pristine CNTs and the inset shows the morphology of the CNTs array; (d) Enlarged SEM image of the CNTs array and the inset shows TEM images of CNTs taken from the stainless steel mesh and catalytic particles used for CNTs growth is evident. The cobalt nanoparticles synthesized in advance was coated to the wire mesh before the CNTs' growth and the ferrocene containing benzene was used as carbon source for the CNTs' growth.



**Figure 3** | SEM images of stainless steel mesh coated with CNT-SO<sub>3</sub>H; (b) Enlarged SEM images of the CNTs arrays; (c) Raman spectra of the CNTs at different stage; (d) C1s, O1s and S2p XPS spectra of the CNT-SO<sub>3</sub>H after sulfonation.

liquids and gases, at different positions of the catalytic column, are taken out for analysis. Figs. 4a and 4b depict respectively the compositions of gas phase and liquid phase at different position along the catalytic column. The concentration of FAME increases with the positions from top to bottom of the catalytic column. Unexpectedly, glycerol, as the main by product of transesterification, is not detected along the catalytic column. The byproducts detected include glyceric acid, glyceraldehyde, 1,1-Dimethoxyhexane, acrolein dimethyl acetal and some short chain alkanes. The quantitative results of analysis on the products taken at the export 8 and the reboiler are listed in Table 2. It is suggested that the glycerol producing by transesterification reaction can further transform into glyceric acid, glyceraldehyde, 1,1-Dimethoxyhexane and acrolein dimethyl acetal by the catalysis on the column.

Noteworthy that the performance of the process is much stable in 100 h of operation, and the morphology of the catalyst appears unchanged after 100 h reaction (Figs. 4c). Comparing with some

results documented on the transesterification of bio oil with methanol, which required a large excess methanol at common conditions<sup>38–40</sup>, the current method possesses overwhelming advantages by intensifying the reaction with simultaneous separation and synchronous transformation of glycerol. The reaction network is elucidated as Fig. 5 and a mathematical model has been developed to describe the current catalytic distillation process for biodiesel production (supporting information and Figs. S1 and S2).

## Discussion

In the catalytic column used in current investigation, multi factors are involved and contribute to the catalytic performance, such as the nanoparticles of cobalt and iron used for growth of carbon nanotubes on stainless steel meshes, the acid centers formed by sulfonation of CNTs and the interactions among them for synergistic effects. The acid centers contribute to the transesterification and dehydration of glycerol and the metallic centers loaded on or encapsulated in the carbon nanotubes contribute to the reactions of dehydrogenation and hydrogenation with methanol. Very recently, Beller et al have reported that the carbon buried metals, such as iron oxide or cobalt, are active for the hydrogenation of nitroarenes to anilines<sup>41,42</sup>. The sum of the factors, intensified by the effect of temporal separation of catalytic distillation, constitutes the high performance process for production of biodiesel and synchronous conversion of glycerol.

As the following development of nano research<sup>43</sup>, the thoughts of meso science are very applicable for catalysis research, which means a kind of complication and includes many more interactions among its nano constituents. The current work includes an integration of catalytic technology, in size from nano, meso to macro reactor and easy to scale up to industrial equipment, to meet the demand on the upgrade of practical industry processes with more efficiency, less emission and energy save.

**Table 1** | Chemical composition of the holistic catalyst on steel mesh analyzed by EDX and the acid density measured by chemical titration using NaOH

Element	CNTs-SH		CNTs-SO <sub>3</sub> H		H <sub>2</sub> SO <sub>4</sub>
	Weight %	Atomic %	Weight %	Atomic %	
C	90.80	95.1	63.3	72.0	—
O	3.20	2.5	28.9	24.6	—
S	6.00	2.4	7.8	3.4	—
Acid density (mmol g <sup>-1</sup> )	—		2.54 (1.98*)		20.4

\*The figures in the parenthesis show the acid density measured by chemical titration after 100 h reaction.



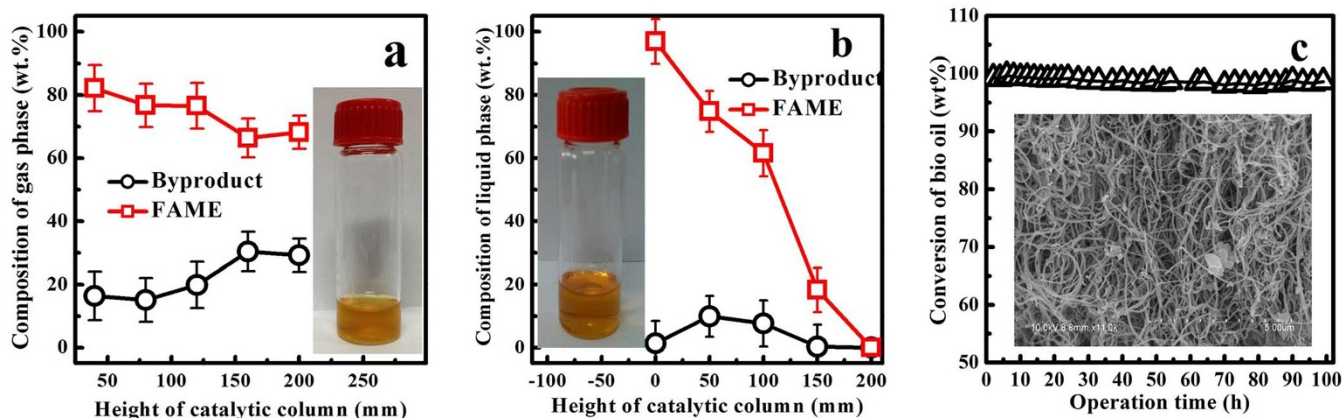


**Figure 4** | (a) The composition of gas phase at the different height of the catalytic column (inset: the photograph of the products at the sample export 8.); (b) The composition of liquid phase at the different position of the catalytic column (inset: the photograph of the products in the reboiler 14.); (c) The variation of bio oil conversion with the operation time in 100 h and inset shows the SEM image of the CNTs on steel mesh after used for about 100 h. (Temperatures: the catalytic column, 493 K; inlet of oil feed (b1), 408 K; inlet of methanol (b2), 388 K; reboiler (14), 388 K; condenser 1, 378 K; condenser 2, fully cooled. Flow rate: oil (b1),  $10.85 \times 10^{-3} \text{ mol} \cdot \text{min}^{-1}$ ; methanol (b2),  $1.73 \times 10^{-3} \text{ mol} \cdot \text{min}^{-1}$ .)

In conclusion, we have demonstrated a design for a catalytic distillation with improved efficiency and enhanced stability for biodiesel production, as well as synchronous conversion of glycerol to a series of high valuable chemicals in situ on the catalytic column of distillation, by well shaped assembling and stabilizing sulfonated carbon nanotubes on stainless steel meshes with cobalt and iron metal nanoparticles in scales from nano, meso to macro reactor. Considering the large quantity of industrial processes adaptive to catalytic distillation, the current integrative design could be built for a broad range of applications. Moreover, by judiciously choosing the further modification of the carbon nanotubes with catalytic functions, we foresee the creation of novel families of catalytic distillation technologies with high efficiency, low emission and energy save.

## Methods

**Pretreatment of the stainless steel meshes.** 316 L stainless steel meshes with wires of 200  $\mu\text{m}$  in diameter were washed by ethanol to remove organic smears and etched in hydrochloric acid for 15 min at 333 K. The treated meshes were then immersed into a sol containing metallic cobalt nanoparticles, which was prepared in advance according to the method similar to that reported in ref. 29. The meshes attached by the cobalt nanoparticles were then dried in vacuum.

**Growth of the CNTs.** The stainless steel meshes coated with Co nanoparticles were loaded in a porcelain boat, which was placed in a horizontal quartz tubular furnace. The meshes were firstly heated to 873 K for 1 h in 10 vol. %  $\text{H}_2/\text{Ar}$  flow to clean the surface for 2 h. When the temperature was ramped to 973 K, 1 wt. % ferrocene containing xylene or benzene (as carbon source) was injected continuously by a syringe and evaporated in the flow for CNTs growth<sup>30</sup>. The growth time was controlled as 1 h in the flowing 10 vol. %  $\text{H}_2/\text{Ar}$  at 973 K.

**Sulfonation.** The stainless steel meshes with CNTs were put into  $\text{Na}_2\text{S}_x$  saturated solution at 358 K under stirring for 24 h for sulfuration of the CNTs as CNTs-SH. Thereafter, hydrogen peroxide was used to oxidize the CNTs-SH to CNTs-SO<sub>3</sub>H at

room temperature. Finally, the sample was thoroughly washed by ethanol and distilled water.

**Catalytic column.** The stainless steel meshes were tailored and shaped as Raschig rings to be loaded in a catalytic column of 20 mm of inner diameter and 200 mm in length, surrounded by a heating furnace. The apparatus for catalytic distillation is shown as Fig. 1.

**Catalytic test.** The bio oil and methanol as the feedstocks were individually injected at the inlets of b1 and b2, respectively, which were heated to different temperatures. The products were obtained at two places when the temperature of the catalytic column was set at 493 K. The first stage of condenser was set at 383 K to recover a part of products from transesterification and the products from the simultaneous conversion of glycerol at the column. The second condenser was fully cooled to recover the methanol, which was fed back to the catalytic column. The reboiler was set at 383 K in order to gain the pure biodiesel from the column bottom. The process was operated continuously. The product samples were analyzed using GC-MS (thermo finnigan trace GC2000 DSQ) equipped with a DB-5MS column (30 m  $\times$  0.32 mm  $\times$  0.25  $\mu\text{m}$ ).

**Characterization.** Laser Raman spectroscopy (Renishaw Invia) was used to characterize the carbon materials. Scanning electron microscope (SEM, LEO1530 VP instrument), transmission electron microscope (TEM, JEM-110) and high resolution transmission electron microscope (HRTEM, JEM-2100) were used to observe the morphologies of the catalysts and the CNTs. X-ray diffraction measurements (XRD) were performed on a Philips X'Pro X-ray diffractometer with Cu K $\alpha$  irradiation ( $\lambda = 0.15418 \text{ nm}$ ). The X-ray source was operated at 40 kV and 40 mA. XPS spectra were obtained under ultra high vacuum ( $<10^{-6} \text{ Pa}$ ) on UIVAC-PHI 5000 Versa Probe with an Al anode (Al K $\alpha = 1486.6 \text{ eV}$ ). All binding energies were calibrated using the

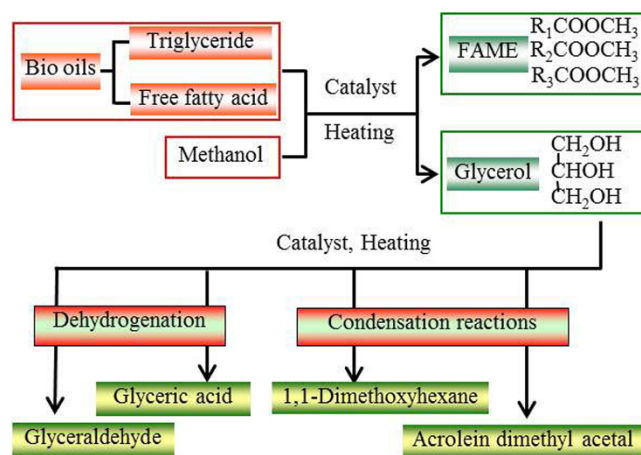


**Figure 5** | The reaction network of transesterification of bio oils with methanol and the in situ transformation of the glycerol.

**Table 2** | The compositions of products at the column top (export 8) and the column bottom (reboiler)

product	Top (wt. %)	Bottom (wt. %)
FAME	68.2	97.0
Glyceraldehyde	1.7	0.2
Glyceric acid	4.3	0.3
Acrolein dimethyl acetal	4.5	0.4
1,1-Dimethoxyhexane	9.3	0.5
Linoleic acid monoester	—	1.1
Others	12.0	0.6

\*The excess methanol is refluxed to the b2 inlet. The product in reboiler is taken out directly without further treatment. The condensate at the export 8 is collected without further treatment.



carbon 1 s as a reference. The sulfur contents of the sulfonated carbon catalysts were determined by elemental analysis using EDX. The acid density of the obtained meshes with CNTs was measured by chemical titration using diluted solution of sodium hydroxide.

- Kiss, A. A. & Bilde, C. S. A review of biodiesel production by integrated reactive separation technologies. *J. Chem. Technol. Biotechnol.* **87**, 861–879 (2012).
- Nguyen, N. & Demirel, Y. Using thermally coupled reactive distillation columns in biodiesel production. *Energy* **36**, 4838–4847 (2011).
- Kiss, A. A., Dimian, A. C. & Rothenberg, G. Biodiesel by catalytic reactive distillation powered by metal oxides. *Energy Fuels* **22**, 598–604 (2008).
- Lotero, E. *et al.* Synthesis of biodiesel via acid catalysis. *Ind. Eng. Chem. Res.* **44**, 5353–5363 (2005).
- Goff, M. J., Bauer, N. S., Lopes, S., Sutterlin, W. R. & Suppes, G. J. Acid-catalyzed alcoholysis of soybean oil. *J. Am. Oil Chem. Soc.* **81**, 415–420 (2004).
- Narvaez, P. C., Rincon, S. M. & Sanchez, F. J. Kinetics of palm oil methanolysis. *J. Am. Oil Chem. Soc.* **84**, 971–977 (2007).
- Baddour, C. E. *et al.* A simple thermal CVD method for carbon nanotube synthesis on stainless steel 304 without the addition of an external catalyst. *Carbon* **47**, 313–318 (2009).
- Konya, Z. *et al.* Large scale production of short functionalized carbon nanotubes. *Chem. Phys. Lett.* **360**, 429–435 (2002).
- Lim, J. K. *et al.* Selective thiolation of single-walled carbon nanotubes. *Synth. Met.* **139**, 521–527 (2003).
- Noiroj, K., Intarapong, P., Luengnarumitchai, A. & Jai-In, S. A comparative study of KOH/Al<sub>2</sub>O<sub>3</sub> and KOH/NaY catalysts for biodiesel production via transesterification from palm oil. *Renew. Energy* **34**, 1145–1150 (2009).
- Macedo, C. C. S. *et al.* New heterogeneous metal-oxides based catalyst for vegetable oil trans-esterification. *J. Braz. Chem. Soc.* **17**, 1291–1296 (2006).
- Xie, W. L. & Li, H. T. Alumina-supported potassium iodide as a heterogeneous catalyst for biodiesel production from soybean oil. *J. Mol. Catal. A Chem.* **255**, 1–9 (2006).
- Talukder, M. M. R. *et al.* Comparison of novozym 435 and amberlyst 15 as heterogeneous catalyst for production of biodiesel from palm fatty acid distillate. *Energy Fuels* **23**, 1–4 (2009).
- Ngaosuwana, K., Lotero, E., Suwannakarn, K., Goodwin, J. G. & Praserttham, P. Hydrolysis of triglycerides using solid acid catalysts. *Ind. Eng. Chem. Res.* **48**, 4757–4767 (2009).
- Ramos, M. J., Casas, A., Rodriguez, L., Romero, R. & Perez, A. Transesterification of sunflower oil over zeolites using different metal loading: A case of leaching and agglomeration studies. *Appl. Catal. A Gen.* **346**, 79–85 (2008).
- Shu, Q. *et al.* Synthesis of biodiesel from waste vegetable oil with large amounts of free fatty acids using a carbon-based solid acid catalyst. *Appl. Energy* **87**, 2589–2596 (2010).
- Kastner, J. R. *et al.* Catalytic esterification of fatty acids using solid acid catalysts generated from biochar and activated carbon. *Catal. Today* **190**, 122–132 (2012).
- Sharma, Y. C., Singh, B. & Upadhyay, S. N. Advancements in development and characterization of biodiesel: A review. *Fuel* **87**, 2355–2373 (2008).
- Toda, M. *et al.* Green chemistry: biodiesel made with sugar catalyst. *Nature* **438**, 178–178 (2005).
- Takagaki, A. *et al.* Esterification of higher fatty acids by a novel strong solid acid. *Catal. Today* **116**, 157–161 (2006).
- Mo, X. H., Lotero, E., Lu, C. Q., Liu, Y. J. & Goodwin, J. G. A novel sulfonated carbon composite solid acid catalyst for biodiesel synthesis. *Catal. Lett.* **123**, 1–6 (2008).
- Shu, Q., Zhang, Q., Xu, G. H. & Wang, J. F. Preparation of biodiesel using s-MWCNT catalysts and the coupling of reaction and separation. *Food. Bioprod. Process.* **87**, 164–170 (2009).
- Rao, B. V. S. K., Mouli, K. C., Rambabu, N., Dalai, A. K. & Prasad, R. B. N. Carbon-based solid acid catalyst from de-oiled canola meal for biodiesel production. *Catal. Commun.* **14**, 20–26 (2011).
- Yu, H., Jin, Y. G., Li, Z. L., Peng, F. & Wang, H. J. Synthesis and characterization of sulfonated single-walled carbon nanotubes and their performance as solid acid catalyst. *J. Solid. State. Chem.* **181**, 432–438 (2008).
- Peng, F., Zhang, L., Wang, H. J., Lv, P. & Yu, H. Sulfonated carbon nanotubes as a strong protonic acid catalyst. *Carbon* **43**, 2405–2408 (2005).
- Park, J. Y., Lee, J. S., Wang, Z. M. & Kim, D. K. Production and characterization of biodiesel from trap grease. *Korean J. Chem. Eng.* **27**, 1791–1795 (2010).
- Simasatitkul, L., Siricharnsakunchai, P., Patcharavorachot, Y., Assabumrungrat, S. & Arpornwichanop, A. Reactive distillation for biodiesel production from soybean oil. *Korean J. Chem. Eng.* **28**, 649–655 (2011).
- Chen, Y. Z., Peng, D. L., Lin, D. X. & Luo, X. L. Preparation and magnetic properties of nickel nanoparticles via the thermal decomposition of nickel organometallic precursor in alkylamines. *Nanotechnology* **18**, 505703 (2010).
- Nakamura, T., Ohana, T., Ishihara, M., Hasegawa, M. & Koga, Y. Chemical modification of single-walled carbon nanotubes with sulfur-containing functionalities. *Diam. Relat. Mater.* **16**, 1091–1094 (2007).
- Wei, S., Kang, W. P., Davidson, J. L. & Huang, J. H. Aligned carbon nanotubes fabricated by thermal CVD at atmospheric pressure using Co as catalyst with NH<sub>3</sub> as reactive gas. *Diam. Relat. Mater.* **15**, 1828–1833 (2006).
- Dong, J., Luo, L., Liang, P. H., Dunaway-Mariano, D. & Carey, P. R. Raman difference spectroscopic studies of dithiobenzoyl substrate and product analogs binding to the enzyme dehalogenase:  $\pi$ -electron polarization is prevented by the C=O to C=S substitution. *J. Raman Spectrosc.* **31**, 365–371 (2000).
- Cech, J. *et al.* Functionalization of multi-walled carbon nanotubes: Direct proof of sidewall thiolation. *Phys. Stat. Sol. (b)* **13**, 3221–3225 (2006).
- Tripathy, S. K. & Yu, Y. T. Spectroscopic investigation of S-Ag interaction in @w-mercaptopentadecanoic acid capped silver nanoparticles. *Spectrochim. Acta Part A* **72**, 841–845 (2009).
- Chwaleba, D., Ilczyszyn, M. M., Ilczyszyn, M. & Ciunik, Z. Glycine-methanesulfonic acid (1 : 1) and glycine-p-toluenesulfonic acid (1 : 1) crystals: comparison of structures, hydrogen bonds, and vibrations. *J. Mol. Struct.* **831**, 119–134 (2007).
- Hueso, J. L., Espinos, J. P., Caballero, A., Cotrino, J. & Gonzalez-Elipe, A. R. *Carbon* **45**, 89–96 (2007).
- Yu, H., Jin, Y. G., Li, Z. L., Peng, F. & Wang, H. J. Synthesis and characterization of sulfonated single-walled carbon nanotubes and their performance as solid acid catalyst. *J. Solid State Chem.* **181**, 432–438 (2008).
- Duesberg, G. S. *et al.* Hydrothermal functionalisation of single-walled carbon nanotubes. *Synth. Met.* **142**, 263–266 (2004).
- Zheng, S., Kates, M., Dube, M. A. & McLean, D. D. Acid-catalyzed production of biodiesel from waste frying oil. *Biomass Bioenergy* **30**, 267–272 (2006).
- Velez, A., Hegel, P., Mabe, G. & Brignole, E. A. Density and conversion in biodiesel production with supercritical methanol. *Ind. Eng. Chem. Res.* **49**, 7666–7670 (2010).
- Reddy, C., Reddy, V., Oshel, R. & Verkade, J. G. Room-temperature conversion of soybean oil and poultry fat to biodiesel catalyzed by nanocrystalline calcium oxides. *Energy and Fuels* **20**, 1310–1314 (2006).
- Jagadeesh, R. V. *et al.* Nanoscale Fe<sub>2</sub>O<sub>3</sub>-based catalysts for selective hydrogenation of nitroarenes to anilines. *Science* **342**, 1073 (2013).
- Westerhaus, F. A. *et al.* Heterogenized cobalt oxide catalysts for nitroarene reduction by pyrolysis of molecularly defined complexes. *Nat. Chem.* **5**, 537 (2013).
- Service, R. F. The next big(ger) thing. *Science* **335**, 1167 (2012).

## Acknowledgments

The authors thank the financial supports from the Ministry of Science and Technology of China (2009CB623504), the National Science Foundation of China (20673054, 21273107), and Sinopec Shanghai Research Institute of Petrochemical Technology.

## Author contributions

D.W.P. conceived, designed and directed the study and the analysis and interpretation of results. Z.D.D., W.D.L. and L.Q. performed catalyst synthesis, characterization and testing. G.X. and G.X.F. participated in data analysis and simulation. X.Z.K. collaborated in mathematic modeling. The manuscript was co-written by D.W.P., Z.D.D. and W.D.L.

## Additional information

Supplementary information accompanies this paper at <http://www.nature.com/scientificreports>

**Competing financial interests:** The authors declare no competing financial interests.

**How to cite this article:** Zhang, D.D. *et al.* High performance catalytic distillation using CNTs-based holistic catalyst for production of high quality biodiesel. *Sci. Rep.* **4**, 4021; DOI:10.1038/srep04021 (2014).



This work is licensed under a Creative Commons Attribution-NonCommercial-NoDerivs 3.0 Unported license. To view a copy of this license, visit <http://creativecommons.org/licenses/by-nc-nd/3.0>